Calibration and Uncertainty Analysis for Modelling Runoff in the Tambo River Basin, Peru, Using Sequential Uncertainty Fitting Ver-2 (SUFI-2) Algorithm

Authors: Carlos Mendoza, Juan Adriel, Chavez Alcazar, Tamar Anaharat, and Zuñiga Medina, Sebastián Adolfo

Source: Air, Soil and Water Research, 14(1)

Published By: SAGE Publishing

URL: https://doi.org/10.1177/1178622120988707

Calibration and Uncertainty Analysis for Modelling Runoff in the Tambo River Basin, Peru, Using Sequential Uncertainty Fitting Ver-2 (SUFI-2) Algorithm

Air, Soil and Water Research
Volume 14: 1–13

DOI: 10.1177/1178622120988707

Juan Adriel Carlos Mendoza, Tamar Anaharat Chavez Alcazar and Sebastián Adolfo Zuñiga Medina

Escuela de Ingeniería Ambiental, Universidad Nacional de San Agustín de Arequipa, Arequipa, Peru.

ABSTRACT: Basin-scale simulation is fundamental to understand the hydrological cycle, and in identifying information essential for water management. Accordingly, the Soil and Water Assessment Tool (SWAT) model is applied to simulate runoff in the semi-arid Tambo River Basin in southern Peru, where economic activities are driven by the availability of water. The SWAT model was calibrated using the Sequential Uncertainty Fitting Ver-2 (SUFI-2) algorithm and two objective functions namely the Nash-Sutcliffe simulation efficiency (NSE), and coefficient of determination (R^2) for the period 1994 to 2001 which includes an initial warm-up period of 3 years; it was then validated for 2002 to 2016 using daily river discharge values. The best results were obtained using the objective function R^2; a comparison of results of the daily and monthly performance evaluation between the calibration period and validation period showed close correspondence in the values for NSE and R^2, and those for percent bias (PBIAS) and ratio of standard deviation of the observation to the root mean square error (RSR). The results thus show that the SWAT model can effectively predict runoff within the Tambo River basin. The model can also serve as a guideline for hydrology modellers, acting as a reliable tool.

KEYWORDS: SWAT model, runoff simulation, Sequential Uncertainty Fitting Ver-2, Nash-Sutcliffe simulation efficiency, Tambo River, semi-arid river basin

RECEIVED: July 1, 2020. **ACCEPTED:** December 29, 2020.

TYPE: Original Research

FUNDING: The author(s) disclosed receipt of the following financial support for the research, authorship, and/or publication of this article: Funding for this work was provided by Universidad Nacional de San Agustin de Arequipa (Nº TP-02-2019-UNSA.), Department of Environmental Engineering (https://www.unsa.edu.pe/).

DECLARATION OF CONFLICTING INTERESTS: The author(s) declared no potential conflicts of interest with respect to the research, authorship, and/or publication of this article.

CORRESPONDING AUTHOR: Juan Adriel Carlos Mendoza, Escuela de Ingeniería Ambiental, Universidad Nacional de San Agustín de Arequipa, Alto Selva Alegre, Arequipa, Peru. Email: jcarlosme@unsa.edu.pe

Introduction

Accurate analysis of the trajectory of water flows from rainfall to streams is essential for the protection and integrated management of water resources.[1] For this, it is essential to understand the physical phenomena that occur within a basin because they represent the relationships found within the system.[2] Hence, hydrological models are an economical and effective tool for the development of almost all water resource management plans.[3]

The main reason for choosing the Soil and Water Assessment Tool (SWAT) model for this study is attributed to its versatility for studies on climate change impacts, sediment transport, simulation of flows, and effects of extreme urbanisation, as well as its flexibility in addressing water resource problems as reported by Gassman et al.[4] The SWAT model is a continuous, spatially semi-distributed, process-based model capable of simulating water balance[5] developed and supported by the Agricultural Research Service of the United States Department of Agriculture (USDA).[6,7]

The calibration process will only be regarded successful if the observation period is representative of the hydrological behaviour of the basin[8] this is essential for calculating sensitive parameters that deserve attention but cannot be directly measured, thus helping to achieve a reliable prediction and to bring about an improvement in performance indices.[9] Therefore, the parameters were optimised and calibrations were carried out using the Sequential Uncertainty Fitting Ver-2 (SUFI-2) algorithm implemented in the SWAT Calibration and Uncertainty Programmes (SWAT-CUP) developed for automatically computing sensitive model parameters.[10] Most SWAT-CUP applications use SUFI-2 algorithm and flow observations to analyse sensitivity, calibration process, and uncertainty of the model.[11] The SUFI-2 algorithm tries to capture as many optimal simulations as possible that are within 95% prediction uncertainty (95PPU). The algorithm does not obtain a unique value for the parameters but an interval that includes all the uncertainties of the processes in the basin.[12]

There is spatio-temporal variability in the distribution of water resources in the Tambo River Basin due to the topography and climatic and hydrological factors of the region.[13] Data on the thermo-pluviometric interactions with other elements that define the climate have determined that there is a water deficit in the lower part and an excess in the headwater region of the Tambo River Basin[14,15] especially in the dry months, due to the diversion of water from a part of the basin to the Pasto Grande hydraulic system.[16] In the headwater region of the Tambo River Basin, the annual volume of water available at 75% persistence is sufficient to meet current demand; however, the monthly balance shows that an average deficit of 23.65 million cubic metres of water exists in the dry season. At the same time, there are 10 other subbasins in the middle and upper part of the Tambo River

Basin with average annual deficits of less than 1.5 million cubic metres of water.[17] Further, droughts, for example the one in 1983, caused estimated losses of USD 200 million in southern Peru[18] and had a critical impact on the water distribution of the region, resulting in agricultural production in southern Peru to fall by up to 75% in 2016.[19,20]

Finally, the flooding in the coastal valleys is a problem that recurs annually, resulting in material- and economic-damage.[19,20] Since 98.7% of the total available water is used for activities within the basin, the implementation of a hydrological model is essential for forecasting the amount of water available. Considering the scarcity of available information, and the location of the basin, it is necessary to carry out a hydrological simulation study of the Tambo River Basin capable of forecasting surface runoff with a reasonable level of precision.

The main objective of this study is to implement the SWAT model for the hydrological simulation of current flow in the Tambo River Basin through the identification and sensitivity analysis of 15 parameters that influence the current generation and the regime of basin flow. The optimal qualitative performance ratings of the SWAT model are defined through model calibration using the SUFI-2 algorithm. The results of this study will help understand the hydrological processes, as well as provide supporting information for the adaptation, management, and planning of the water resources of the Tambo River Basin.

Materials and Methods

Study area

The Tambo River Basin is located between latitudes 16° 00'S and 17° 15' S, and longitudes 70° 30'W and 72° 00'W in the south of Peru at 3900 m above sea level, and includes the provinces of Mariscal Nieto, Sánchez Cerro, Islay and San Román.

The basin extends over 13 361 km^2, and the river – from its source to the mouth – is 289 km long; its main tributaries are Carurnas, Coralaque, Ichuña, and Paltature. The surface water resources of the Tambo River Basin are generated in the upper basin, with a total annual volume of 1077 million cubic metres and an average annual discharge of 31 457 m^3/s.[21] The population of the Rio Tambo Basin is concentrated in urban and rural areas including the Mollendo and Ubinas Districts. The main productive activities of its population are agriculture and livestock rearing.[22]

The basin is characterised by variable thermal conditions, and three types of climate have been identified based on the Köppen criteria: very dry semi-warm climate (desert or subtropical arid) with average annual rainfall of 150 mm and average annual temperatures of 18°C to 19°C, temperate subhumid climate (Steppe and low inter-Andean valleys) with temperatures exceeding 20°C and annual precipitation below 200 mm, and cold or boreal climate (Meso-Andean Valleys) characterised by average annual precipitation of 300 mm and annual temperatures less than 12°C.[21] In the basin, land without vegetation predominates, with small snow-capped mountains also found in the upper reaches; in the south, the Pasto Grande reservoir contributes 7.4 hm^3 annually during the dry season from September to December.[15]

The model – SWAT

The free software, the SWAT (2012), is a rainfall-runoff model of semi-distributed parameters, capable of simulating various physical processes on a continuous time scale (annual, monthly, and daily). The main objective of the model is to predict the impact of management on water and sediments in hydrographic basins, as well as the impact of agricultural management practices on water quality (nutrients and pesticides). It provides results with reasonable precision in large basins with a variety in relief, as well as in types and uses of soils. Its high spatial resolution allows it to be implemented at both continental and hydrological basin scales.[5,6] The hydrological component of SWAT allows the calculation of elements of the water balance and consequently, the water resources (blue, green water, etc.) even at the sub-basin level. The terrestrial phase of the hydrological cycle is simulated based on the following water balance equation (equation [1])

$$SW_t = SW_0 + \sum_{i=1}^{t}\left(R_{day} - Q_{surf} - E_a - w_{seep} - Q_{gw}\right) \qquad (1)$$

where SW_t and SW_0 are the final and initial soil moisture contents (mm H_2O), t is time in days, R_{day} is the amount precipitation on day i (mm H_2O), Q_{surf} is the amount of surface runoff on day i (mm H_2O), Ea is the amount evapotranspiration on day i (mm H_2O), w_{seep} is the amount water seepage from the vadose zone into the soil profile on day i (mm H_2O), and Q_{gw} is the amount of return flow on day i (mm H_2O).[7]

Data used

Topography information (Figure 1A) and the greater land-use capacity map (Figure 2) were obtained from the GeoServer of the Ministry of the Environment of Peru.[23] The soil map (Figure 3) was extracted from the website of the Food and Agriculture Organisation.[24] Input data for the SWAT meteorological generator such as maximum and minimum daily temperature and daily precipitation for the period 1994 to 2016 were obtained from Servicio Nacional de Meteorología e Hidrología del Peru,[25] while the wind speed, solar radiation, and relative humidity were simulated by the SWAT Model; flow data for the period 1994 to 2016 required for the calibration (Figure 1B) were obtained from Autoridad Nacional del Agua.[26] Detailed information on the input variables used is given in Table 1.

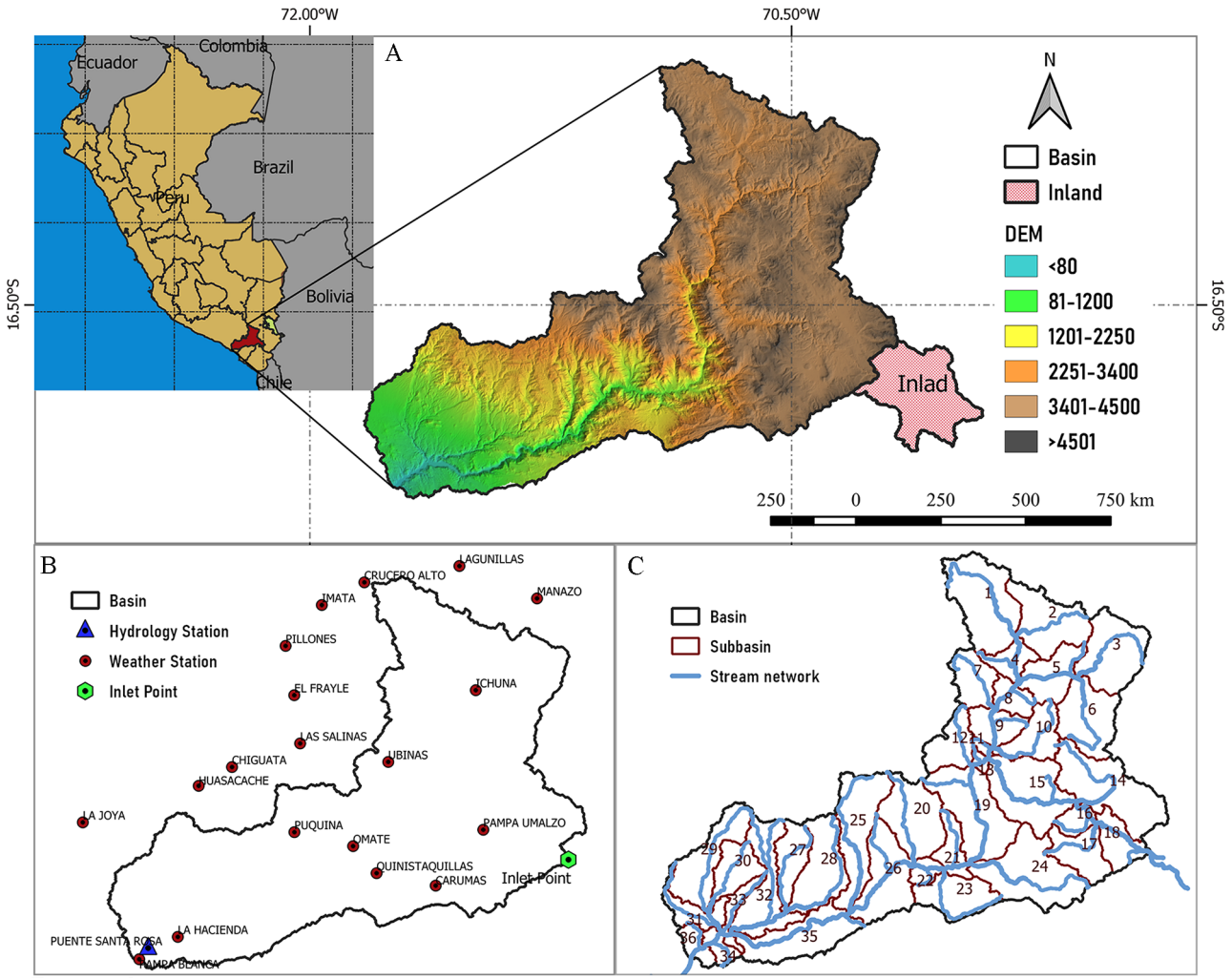

Figure 1. (A) Location map of the Tambo River Basin and 30 m DEM, (B) location of meteorological stations in the basin and (C) flow-path and sub-catchment delineation map.
Abbreviation: DEM, Digital elevation model.

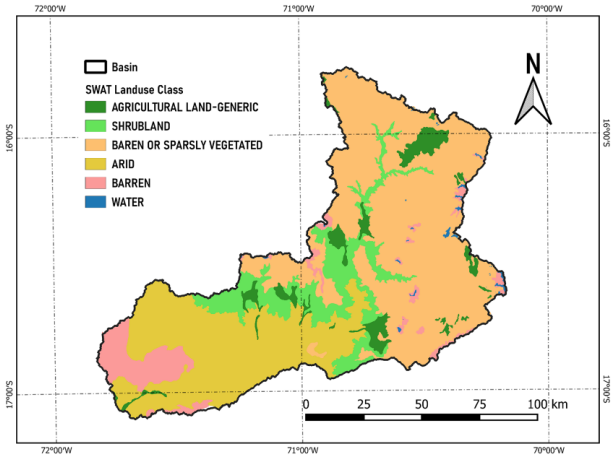

Figure 2. Land-use map of the Tambo River Basin.

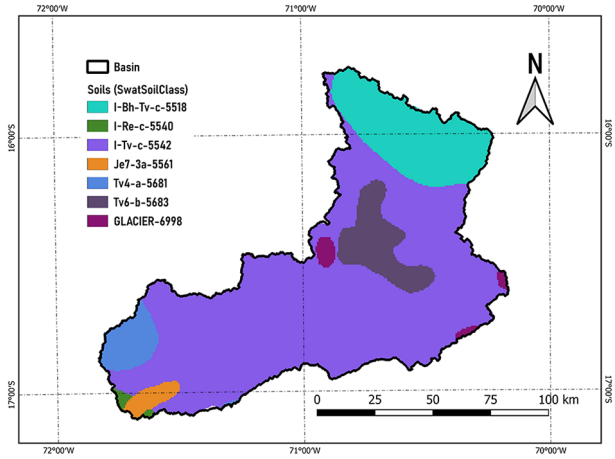

Figure 3. Soil map of the Tambo River Basin.

SWAT set-up

The SWAT model was set up with the help of the ArcGIS interface version of SWAT (ArcSWAT 2012). Initially, delineation of the basin and sub-basins was carried out based on topography to generate flow direction, flow accumulation, and stream networks. The delineation generated 36 sub-basins (Figure 1C) through the selection of outlets and inlet points of the basin. The next step was the creation of hydrologic response units (HRUs) based

Table 1. Input variables used for SWAT modelling.

INPUT DATA	DESCRIPTION	SOURCE
Extreme temperature	Minimum and maximum daily Temperature. Period: 1994-2016. 19 stations.	The National Service of Meteorology and Hydrology of Peru (SENAMHI) https://www.senamhi.gob.pe/
Precipitation	Daily precipitation. Period: 1994-2016. 19 stations.	
DEM	Digital elevation model (30 m resolution)	GeoServidor Ministry of the Environment of Peru (MINAM) http://geoservidorperu.minam.gob.pe/
Land use	Resolution 30 m	
Soil type	Resolution 10 km	The Food and Agriculture Organisation of the United Nations (FAO) http://www.fao.org/
River discharge and point inlet	Daily river discharge. Period: 2001-2016.	Autoridad Nacional del Agua (ANA) https://www.ana.gob.pe/

Abbreviations: ANA, Autoridad Nacional del Agua; DEM, Digital elevation model; FAO, Food and Agriculture Organisation of the United Nations; MINAM, GeoServidor Ministry of the Environment of Peru; SENAMHI, National Service of Meteorology and Hydrology of Peru; SWAT, Soil and Water Assessment Tool.

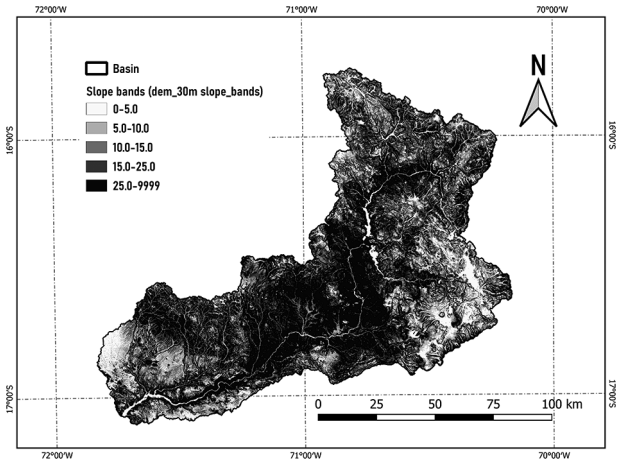

Figure 4. Slope map of the Tambo River Basin.

on differences in the properties of soil, land use, and slope, of each section of the sub-basin. However, the number of HRUs generated depend on filtration based on the thresholds specified.

In this case, 598 HRUs were generated that maintained as accurate a spatial variability as was possible with threshold values of 2% for both land use and soil type, and 5% for slope, compared to most parameters related to SWAT where thresholds values are greater than 5%. Furthermore, this research used five slope classes defined as 0% to 5%, 5% to 10%, 10% to 15%, 15% to 25%, and > 25% (Figure 4), based on a study conducted by Niraula et al[27] for a semi-arid basin. The model was built for the period 1994 to 2016. The Pasto Grande reservoir is within the basin in the south-east of Peru; a spillway from the Pasto Grande reservoir which discharges water from September to December was considered an inlet point for water, from 2001. While preparing the input tables, it was ensured that all meteorological data (precipitation, relative humidity, temperature, wind speed, and solar radiation) were represented in the SWAT model. After completing the above-mentioned steps, the model was ready to run at the default parameter settings.

Description of SUFI-2 algorithm in SWAT-CUP

Calibration using the SUFI-2 algorithm is performed with a series of iterations including numerous simulations, with each iteration fed with the results of the previous one. This results in achieving an approximate (optimised) simulated variable. The results of the iterations are a set of values (ranges) assigned to the parameters that describe the hydrological processes, physical characteristics, and dynamics of each hydrographic basin. Each new iteration presents intervals (ranges) of the parameters recursively closer to their real value. This aims to limit the uncertainty in the initial ranges of the parameters as measurements of these are often not available.[28,29] Thus, based on the flow measurements introduced in SUFI-2, each successive iteration provides greater accuracy in the ranges of the parameters of each study area. This procedure is called reverse hydrological modelling.[12,28,30] To calculate the sensitivities of the response parameters with the technique specified by the modeller, an objective function must be defined.[31] Different methods of defining an objective function may lead to different results[32]; different objective functions, for example, the coefficient of determination (R^2) and the Nash-Sutcliffe simulation efficiency (NSE), which have been defined to reduce the problem of non-uniqueness in model characterization,[33] this is because NSE generates parameter values similar to other objective functions.[34]

Sensitivity analysis

Sensitivity analysis is performed to identify the most important parameters of the model, and is carried out based on changes to the objective function depending on the interactions among

parameter values. These changes are called relative sensitivities. Then, a linear approximation of the model parameters is made in agreement with the sensitivity of the objective function. Furthermore, the level of significance between the parameters is determined based on the *t*-test and *P*-value. Lower absolute values of the *t*-test are less sensitive than larger values, while the *P*-values greater than 0.05 are of less importance than values closer to zero.[35]

All of these procedures are developed in SWAT-CUP. The selection of 15 parameters (CN2, ALPHA_BF, GW_DELAY, GWQMN, GW_REVAP, REVAPMN, RCHRG_DP, ESCO, EPCO, SLSUBBSN, OV_N, SOL_BD, CH_K2, CH_N2, TRNSRCH) for this study was carried out based on the study by Lévesque et al[36] which identified 34 parameters that are sensitive to flow. New parameters in addition to this study were also included based on investigations related to semi-arid zones.

Calibration and validation

The calibration process consists of adjusting the model parameter values so the simulated values approach those observed. It is important to understand that the hydrological model does not know the initial simulation conditions, therefore a warm-up period is required.[37] The readings from the calibrated model explain the uncertainties which are evaluated by the *P*-factor and *R*-factor, the *P*-factor being the percentage of simulation within the 95% prediction uncertainty (95PPU). The R-factor is the average thickness of the 95PPU band divided by the standard deviation of the data. The suggested values for the *P*-factor and *R*-factor are '>0.7' and '<1.5', respectively.[12,28,38]

In the validation process, the parameter values determined during the calibration process were used. The simulation should be performed with data used in the calibration process[39,40] to ensure that if the model demonstrates a satisfactory performance during the validation process, it will represent the physical conditions of the basin.[41] SWAT calibration and validation was processed with the SUFI-2 algorithm included in the SWAT-CUP.[38] A divided sample procedure that uses runoff data from the Puente Santa Rosa bridge station for the period 1994 to 2001 and 2002 to 2016 was employed in most calibrations using the SUFI-2 algorithm. Throughout the calibration and validation process, 3 years (1994-1996) were considered as a warm-up period to ensure better performance as the initial conditions of the system are unknown to the model. Multiple simulation iterations were executed, with a minimum of 500 simulations in every execution.

Model performance evaluation

In this study, the NSE, R^2, percent bias (PBIAS), and root mean square error (RSR) were the four performance measures used to evaluate the performance of the hydrological model. These performance measures were recommended by Moriasi et al[42] who specified the evaluation criteria.

NSE is one of the most commonly used performance criteria in hydrology; it varies from $-\infty - 1$, exhibiting better values in the range 0.5 to 1. NSE determines the relative magnitude of the residual variance in comparison with the observed data variance, and is calculated using equation (2)

$$NSE = 1 - \frac{\sum_{i=1}^{n}\left(Q_{mo} - Q_{ss}\right)_i^2}{\sum_{i=1}^{n}\left(Q_{mo,i} - \bar{Q}_{me}\right)^2} \tag{2}$$

where Q_{me} is the mean of observed discharges, Q_{mo} is the observed discharge, Q_{ss} is the simulated discharge, and n is the total number of observations.

The collinearity between the simulated and observed flow rates is determined using R^2; the values vary from 0 to 1, with values greater than 0.5 representing good performance. R^2 calculated using equation (3) as follows

$$R^2 = \frac{\left[\sum_{i=1}^{n}\left(Q_{mo,i} - \bar{Q}_{mo}\right)\left(Q_{ss,i} - \bar{Q}_{ss}\right)\right]^2}{\sum_{i=1}^{n}\left(Q_{mo,i} - \bar{Q}_{mo}\right)^2 \sum_{i=1}^{n}\left(Q_{ss,i} - \bar{Q}_{ss}\right)^2} \tag{3}$$

PBIAS measures the average tendency of the simulated data. Abbaspour et al[38] suggests that PBIAS values must approach 0 or should be less than 25% for the model to be considered a good model. Positive values indicate underestimation of the model and negative values indicate overestimation of the model.[43] It can be calculated as follows (equation [4])

$$PBIAS = 100 \times \frac{\sum_{i=1}^{n}\left(Q_{mo} - Q_{ss}\right)_i}{\sum_{i=1}^{n} Q_{mo,i}} \tag{4}$$

where Q_{mo} is the observed discharge and Q_{ss} is the simulated discharge.

The standard deviation index represented by RSR is the mean squared error index (RMSE) divided by the standard deviation of the observed data. It may take values from 0 to ∞,[42] with values less than 0.7 indicating good simulation.[44,45] RSR can be calculated as follows (equation [5])

$$RSR = \frac{\sqrt{\sum_{i=1}^{n}\left(Q_{mo} - Q_{ss}\right)_i^2}}{\sqrt{\sum_{i=1}^{n}\left(Q_{mo,i} - \bar{Q}_{me}\right)^2}} \tag{5}$$

where Q_{me} is the mean of observed discharges, Q_{mo} is the observed discharge, Q_{ss} is the simulated discharge, and n is the total number of observations. The optimal ranges of the parameters are provided in Table 2.

Table 2. Classification of statistical indices.

NSE	PBIAS	R^2	RSR	CLASSIFICATION
$0.75 < NSE \leq 1.00$	$PBIAS \leq \pm 10$	$0.75 < R^2 \leq 1.00$	$0.00 \leq RSR \leq 0.50$	Very good
$0.60 < NSE \leq 0.75$	$\pm 10 < PBIAS \leq \pm 15$	$0.60 < R^2 \leq 0.75$	$0.50 \leq RSR \leq 0.60$	Good
$0.36 < NSE \leq 0.60$	$\pm 15 < PBIAS \leq \pm 25$	$0.50 < R^2 \leq 0.60$	$0.60 \leq RSR \leq 0.70$	Satisfactory
$0.00 < NSE \leq 0.36$	$\pm 25 < PBIAS \leq \pm 50$	$0.25 < R^2 \leq 0.50$	$RSR > 0.7$	Bad
$NSE \leq 0.00$	$\pm 50 \leq PBIAS$	$R^2 \leq 0.25$		Inappropriate

Moriasi et al[45], Fernandez et al[46], Van Liew et al[47].
Abbreviations: NSE, Nash-Sutcliffe simulation efficiency; PBIAS, percent bias; RSR, root mean square error.

Results and Discussion

Parameter sensitivity analysis

The results of the sensitivity analysis of 15 parameters with respect to model output are provided in Table 3, which summarises the parameter sensitivity concerning surface flow, base flow, and streamflow, as well as the initial values and best ranges of model parameters. The results of the global sensitivity analysis with the *t*-test indicate the most sensitive parameters ($P < 0.05$).

For the objective function NSE, the fraction of transmission losses from the main channel that enters the deep aquifer (TRNSRCH, $P = 0.00$, $t = -18.51$) was found to be the most sensitive parameter followed by effective hydraulic conductivity of the soil layer (CH_K2, $P = 0.00$, $t = -11.84$), groundwater delay (days) (GW_DELAY, $P = 0.026$, $t = -2.218$), deep aquifer percolation fraction (RCHRG_DP, $P = 0.03$, $t = -2.159$), and Manning's *n* value for overland flow (OV_N, $P = 0.04$, $t = 2.024$) for the calibration process.

For the objective function R^2, the fraction of transmission losses from the main channel that enters the deep aquifer (TRNSRCH, $P = 0.00$, $t = -24.48$) was identified as the most sensitive parameter followed by curve number II (CN2, $P = 0.00$, $t = -9.23$), deep aquifer percolation fraction (RCHRG_DP, $P = 0.00$, $t = -4.52$), effective hydraulic conductivity in main channel alluvium (mm/h) (CH_K2, $P = 0.00$, $t = -3.94$), groundwater delay (days) (GW_DELAY, $P = 0.00$, $t = -3.43$), Manning's 'n' value for the channel (CH_N2 $P = 0.00$, $t = 3.26$), ground water re-evaporation coefficient (GW_REVAP, $P = 0.04$, $t = -2.02$), and base flow recession constant (ALPHA_BF, $P = 0.05$, $t = -1.93$), for the calibration process. A dotty plot (Figures 5 and 6) is the plot of parameters based on the objective function that indicates a distribution of the sampling points that explain the parameter sensitivity.[38] The greatest number of points of the R^2 objective function are in the optimal interval ($R^2 > .5$).

In a sensitivity analysis using both objective functions, the fraction of transmission losses from the main channel that enters the deep aquifer (TRNSRCH) was the most sensitive parameter. Sensitivity analysis using R^2 does not suggest the Manning's *n* value for overland flow (OV_N) as a sensitive parameter, but introduces four new sensitive parameters (CN2, CH_N2, ALPHA_BF, GW_REVAP).

The sensitive parameters are related to the configuration of the lateral flow in the root zone, the connection of the shallow aquifer to the river bed, and dynamics of groundwater recharge, pointing to the importance of the relationship between the shallow aquifer and the main channel. The sensitive parameters (CN2, ALPHA_BF, RCHRG_ GW and CH_K2) observed for semi-arid basins in Turkey, South Africa,[48] Spain, France, and China are similar to the those indicated for R^2.

Some sensitive parameters are related to the transport and transmission processes in the main channels (TRNSRCH, OV_N, CH_N2) due to the unique characteristic of the basin that results in greater intensity of precipitation in the headwaters of the basin where there is greater flow, with large amounts of water transported several kilometres towards the downstream end of the basin. The comparison of the NSE and R^2 objective functions using SUFI-2 indicates that better results are obtained using R^2.

Calibration and uncertainty analysis

Before calibration, the model was incapable of simulating streamflow values, and showed poor index values of $R^2 = 0.48$, NSE = -0.98, PBIAS = -162, and RSR = 1.41, necessitating the calibration process and automated analysis of flow uncertainty to improve the indices.

The sensitive parameters were continuously modified for the daily and monthly values for the period 1994 to 2001 using SUFI-2 algorithm with 500 simulations for each execution. The measured and predicted results were correlated at the same time with the output end, FLOW_OUT_34 (subbasin 34).

During the calibration, the *P*-factor and *R*-factor obtained were 0.98 and 1.18, respectively, for the two

Table 3. Sensitivity ranking of SWAT model parameters in the Tambo River basin catchment.

PARAMETER NAME	DESCRIPTION	INITIAL RANGE	OBJECTIVE FUNCTION NSE				OBJECTIVE FUNCTION R^2			
			RANK	FITTED VALUE	*T*-STAT	*P*-VALUE	RANK	FITTED VALUE	*T*-STAT	*P*-VALUE
v__TRNSRCH.bsn	Fraction of transmission losses from main channel that enters deep aquifer	0 to 1	1	0.197	-18.51	0.00	1	0.153	-24.48	0.00
v__CH_K2.rte	Effective hydraulic conductivity in main channel alluvium (mm/h)	0 to 100	2	45.700	-11.84	0.00	4	66.3	-3.94	0.00
v__GW_DELAY.gw	Groundwater delay (days)	5 to 50	3	5.315	-2.21	0.02	5	10.355	-3.43	0.00
v__RCHRG_DP.gw	Deep aquifer percolation fraction	0.4 to 1	4	0.495	-2.15	0.03	3	0.605	-4.52	0.00
r__OV_N.hru	Manning's n value for overland flow	-0.1 to 0.1	5	-0.061	2.02	0.04	13	0.007	0.42	0.67
r__CN2.mgt	Curve number II	-0.3 to 0.1	6	-0.175	-1.49	0.13	2	-0.042	-9.23	0.00
r__SOL_BD().sol	Baseline flow recession constant (days)	-0.2 to 0.2	7	0.138	-1.27	0.20	15	-0.080	-0.31	0.75
v__GW_REVAP.gw	Ground water re-evaporation coefficient	0.01 to 0.3	8	0.184	-1.21	0.22	7	0.192	-2.02	0.04
v__CH_N2.rte	Manning's 'n' value for the channel	0 to 1	9	0.677	0.96	0.33	6	0.873	3.26	0.00
v__REVAPMN.gw	Threshold depth of water in the shallow aquifer for re-evaporation to occur (mm)	15 to 60	10	30.075	0.65	0.51	14	51.765	-0.39	0.69
v__ESCO.bsn	Soil evaporation compensation factor	0.5 to 0.9	11	0.716	0.42	0.66	10	0.83	1.26	0.20
v__ALPHA_BF.gw	Base flow recession constant	0.5 to 0.85	12	0.812	0.40	0.68	8	0.733	-1.93	0.05
r__SLSUBBSN.hru	Average slope length (m)	-0.2 to 0.2	13	-0.160	-0.36	0.71	12	-0.013	-0.49	0.62
v__GWQMN.gw	Threshold depth of water in the shallow aquifer required for return flow to occur (mm)	500 to 1600	14	947.700	0.2569	0.7974	9	782.7	-1.4461	0.1488
v__EPCO.bsn	Plant uptake compensation factor	0.4 to 0.8	15	0.694	0.1728	0.8629	11	0.654	0.7205	0.4716

Abbreviation: SWAT, Soil and Water Assessment Tool.
[a]r_ refers to a relative change in the parameters where their current values are multiplied by (1 plus a factor in the given range).
[b]v_ refers to the substitution of a parameter value by another value in the given range.[28]
Note. The shaded regions in the above table are most important for calibration.

objective functions. The final results were good, as expected, and the ratio of *P*-factor to *R*-factor was high (greater than 1 for SUFI-2) for a typical uncertainty analysis, indicating acceptable performance of the uncertainty analysis in this study.[31,49,50]

The performance indices have different values in the daily and monthly simulations. When NSE is the objective function, the values of NSE, R^2, PBIAS, and RSR are 0.69, 0.70, 14.7, and 0.55, respectively, for calibration of daily time series simulation. The values indicate that the SWAT model could be used

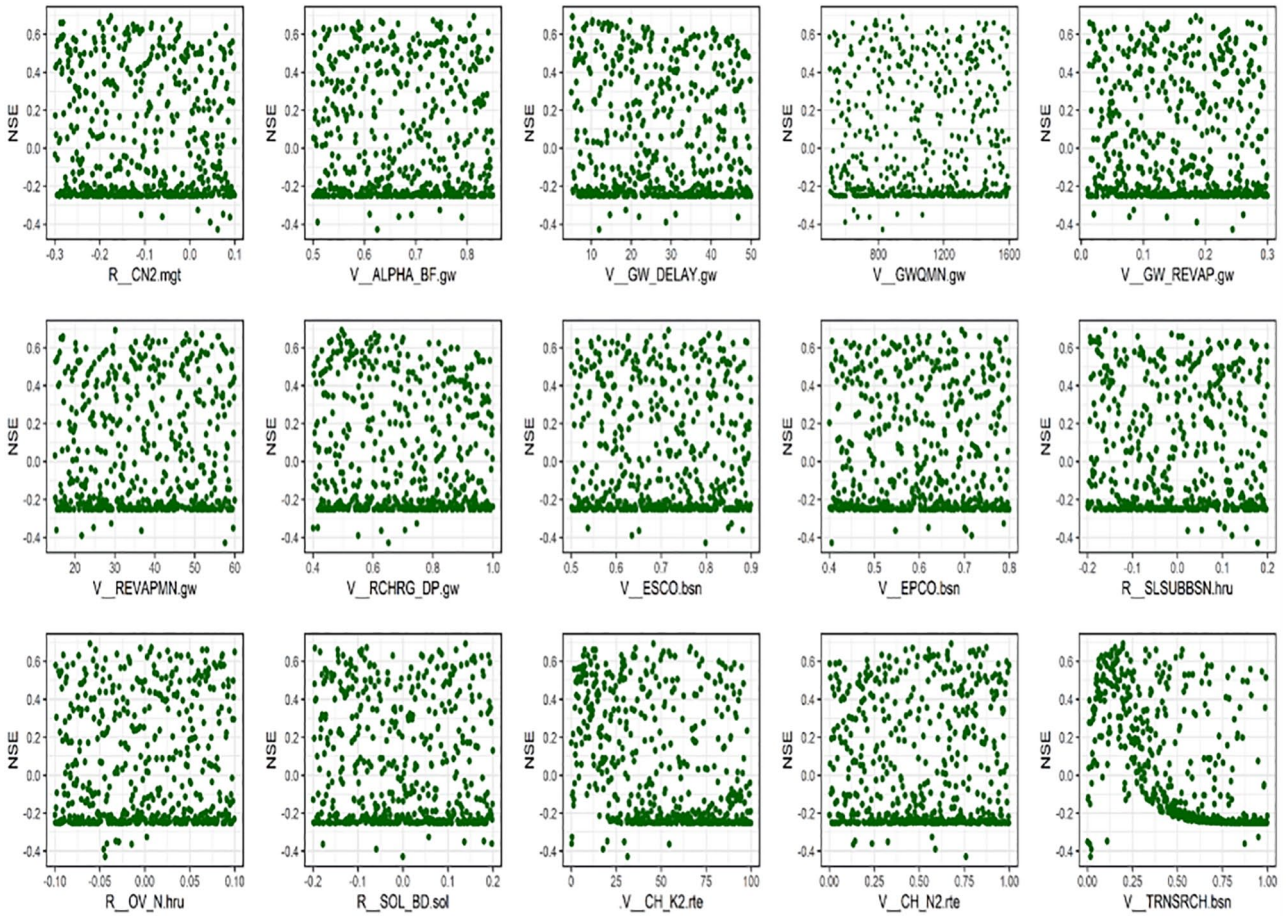

Figure 5. Dotty plots with objective function of NSE coefficient against each aggregate SWAT parameter.
NSE indicates Nash-Sutcliffe simulation efficiency; SWAT, Soil and Water Assessment Tool.

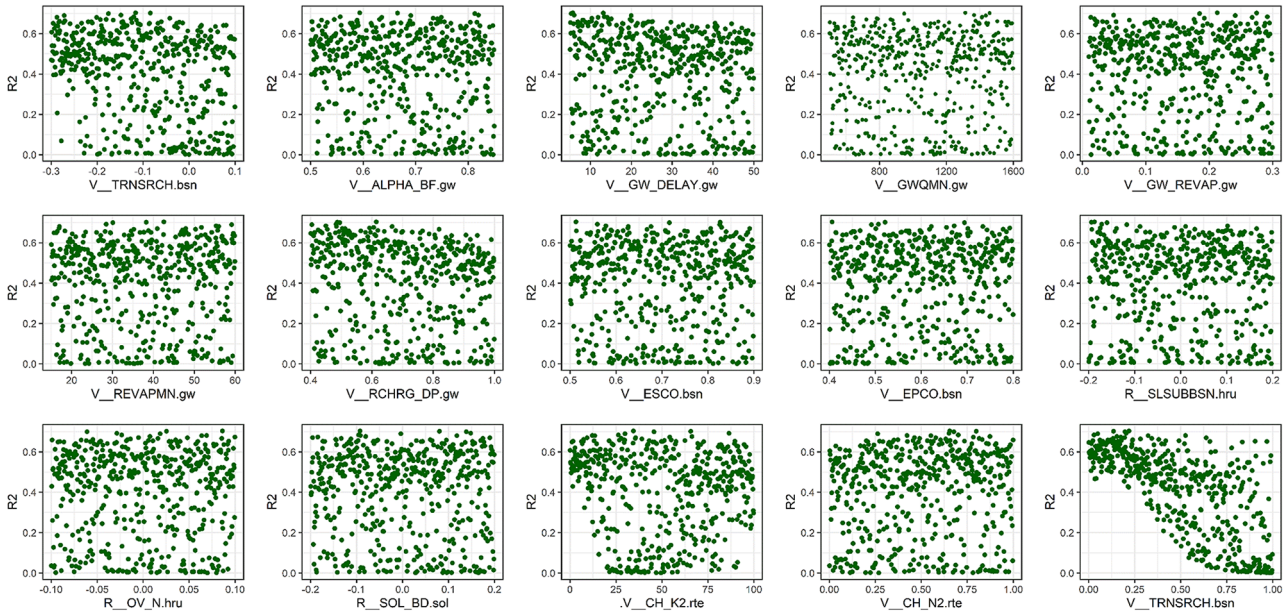

Figure 6. Dotty plots with objective function of R^2 coefficient against each aggregate SWAT parameter.
SWAT indicates Soil and Water Assessment Tool.

with good results for simulations in this area. Table 2 categorises these results as Good. When R^2 is the objective function, the values of NSE, R^2, PBIAS, and RSR are 0.65, 0.65, 5.3, and 0.59, respectively, for calibration of the daily time series simulation. According to Table 2, these results are Good (NSE, R^2, and RSR) and Very Good (PBIAS). The hydrograph of daily

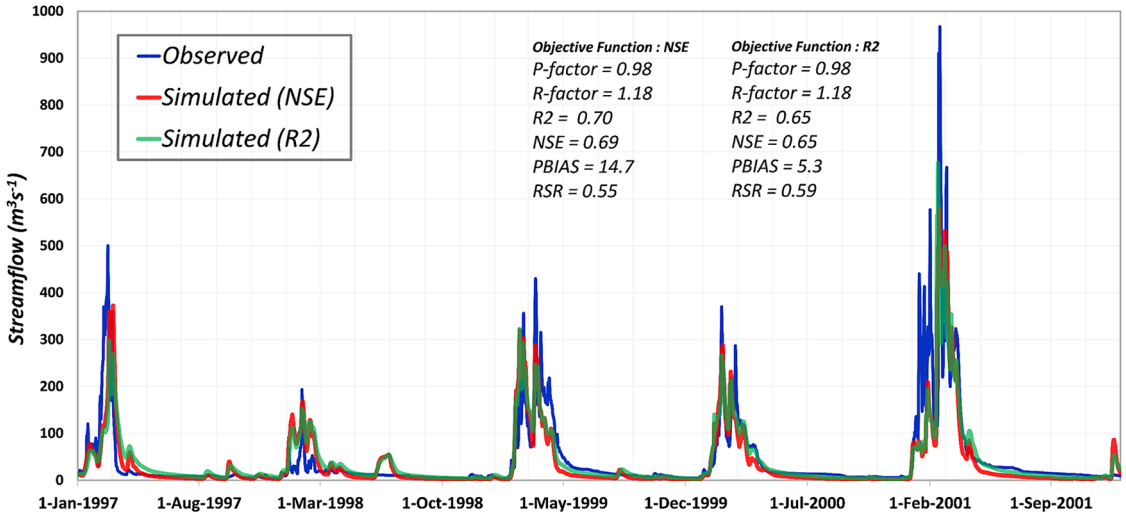

Figure 7. Hydrograph of simulated and observed daily flow using two objective functions for calibration period.
NSE indicates Nash-Sutcliffe simulation efficiency; PBIAS, percent bias; RSR, root mean square error.

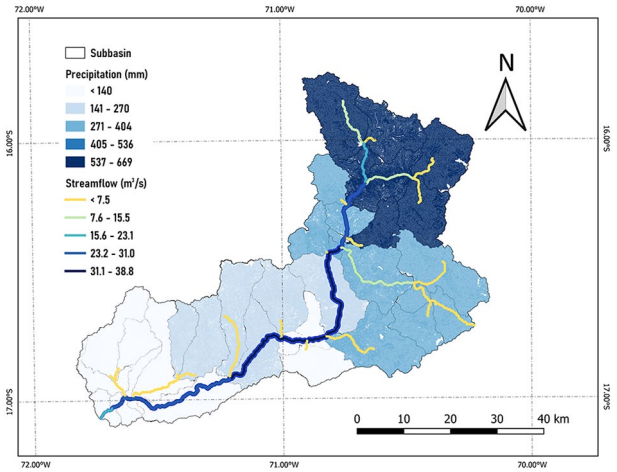

Figure 8. Precipitation and water discharge distribution of the Tambo River Basin.
NSE indicates Nash-Sutcliffe simulation efficiency; PBIAS, percent bias; RSR, root mean square error.

simulation using the two objective functions is presented in Figure 7.

The calibration of monthly simulation produces better values for output than daily simulation. When NSE is the objective function, the values of NSE, R^2, PBIAS, and RSR in the monthly simulation are 0.86, 0.87, 14.4, and 0.38, respectively. Table 2 categorises these results as Very Good (NSE, R^2, and RSR) and Good (PBIAS), indicating that the model could describe hydrological processes very well for monthly simulations. When R^2 is the objective function, the values of NSE, R^2, PBIAS, and RSR in the monthly simulation are 0.84, 0.85, 4.45, and 0.39, respectively. According to Table 2, these results are Very Good, indicating that the model could describe hydrological processes very well for monthly simulations. However, the model simulated lower streamflow in the catchment, particularly during May to October, than what was observed. This could be attributed to considerable land use changes in this period due to the high intensity of precipitation in headwaters of the basin (Figure 8), and the resulting abundant growth of vegetation is areas classified as barren or sparsely vegetated – which begin to disappear when the precipitation decreases – changing CN2 and OV_N. These phenomena are not considered in the SWAT model as there is no variation seen in the land-use maps. The hydrograph of monthly simulation for the two objective functions is presented in Figure 9, and the scatter plot of the monthly simulation for the two objective functions is presented in Figure 10. The calibrated parameter ranges were later used in validation. The adjusted values and the best final distribution of parameters are represented in Table 3.

Model validation

Model validation is performed to check the accuracy of the output representation with reference to the actual streamflow data. The validation of the model was done by comparing the observed and simulated data. The model validation process for both daily and monthly simulations was conducted from 2002 to 2016. Daily flow validation using the NSE function resulted in NSE, R^2, PBIAS, and RSR values of 0.52, 0.67, 5.89, and 0.69, respectively. As can be seen in Table 2, these results can be categorised as Satisfactory (NSE and RSR), Good (R^2) and Very Good (PBIAS). For function R^2 function the values of NSE, R^2, PBIAS, and RSR were 0.64, 0.67, -1.31, and 0.60, respectively. As indicated in Table 2, these results can be categorised as Good (NSE, R^2, and RSR) and Very Good (PBIAS). For daily flow simulation, the model performed did not well during the validation period compared with during the calibration

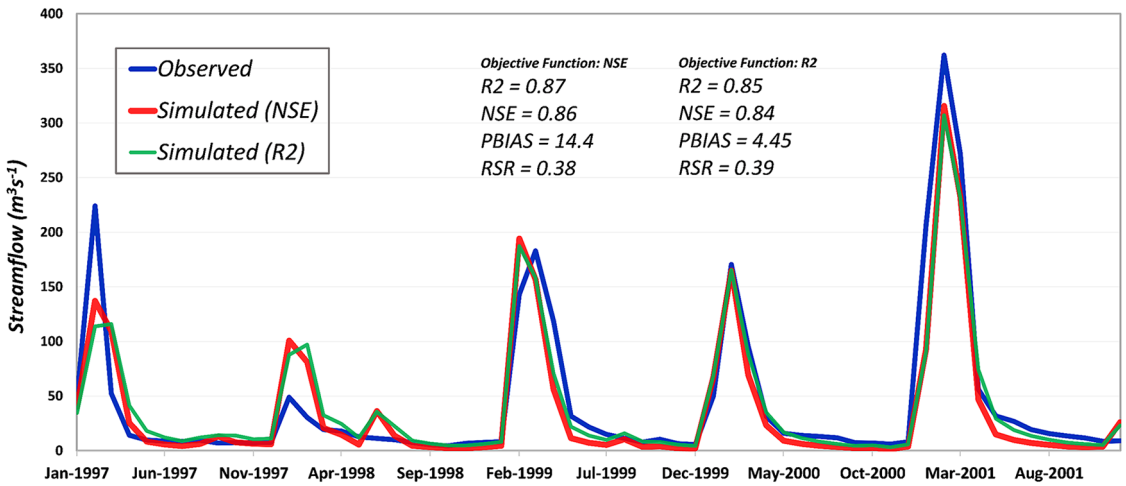

Figure 9. Hydrograph of simulated and observed monthly flow using two objective functions for calibration period.
NSE indicates Nash-Sutcliffe simulation efficiency; PBIAS, percent bias; RSR, root mean square error.

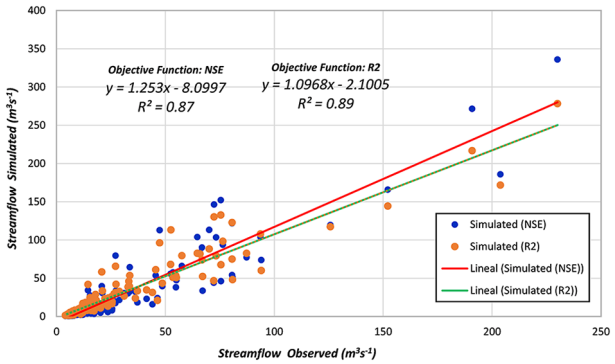

Figure 10. Scatter plot for monthly simulation using two objective functions for calibration period.
NSE indicates Nash-Sutcliffe simulation efficiency.

period when using NSE as the objective function. With R^2 objective function, the values obtained for indices during validation are close to the values obtained during calibration. However, there is improvement in the PBIAS for both NSE and R^2 objective functions. The hydrograph of daily simulation using the two objective functions is presented in Figure 11.

The NSE, R^2, PBIAS, and RSR values from monthly flow validation using NSE as the objective function were 0.70, 0.87, 5.87, and 0.55, respectively. According to Table 2, the results can be categorised as Good (RSR and NSE) and Very Good (PBIAS and R^2). When R^2 is the objective function, NSE, R^2, PBIAS, and RSR values were less than during calibration, and were 0.85, 0.89, -1.6, and 0.39, respectively. As seen in Table 2, the results can be categorised as Very Good. For the monthly simulation, the model remained in the same category (Good) as in the calibration period when NSE was the objective function, while with R^2, the indices exhibited better values than the values obtained in the calibration process. The hydrograph and scatter plot of the monthly simulation using the two objective functions, are presented in Figures 12 and 13, respectively.

Conclusion

This study examined the possibility of using the SWAT model to accurately predict the daily discharge in a river basin. The model was implemented for the Tambo River catchment located in southern Peru in South America. Model calibration and parameter uncertainty analysis were conducted simultaneously using the SUFI-2 algorithm for two objective functions, NSE and R^2; the algorithm was implemented in SWAT-CUP which is a standalone model that includes several graphical modules. Monthly simulation provides better results than daily simulation. For both daily and monthly simulations, higher performance was achieved using objective function R^2 compared to NSE; SWAT-CUP revealed a better value of R^2 with a Bad performance rating for PBIAS, which means having to choose a lower value of R^2 for better results.

The objective function R^2 found more sensitive parameters in the sensitivity analysis compared with NSE. The sensitive parameters found by R^2 are similar to those found in related studies for semi-arid areas. For the sensitivity analysis during calibration, both the objective functions R^2 and NSE must be used to obtain the two sets of parameters that calibrate the model to evaluate which of the parameters best represent the physical conditions of the basin.

The process of modelling streamflow becomes even more difficult in catchments where there is irregular rainfall distribution. In addition, the lack of continuous high-quality data, especially in Peru, is a challenge that hydrologists face when modelling streamflow. Land-use and soil types are the most important data needed for the definition of HRUs; any effort to obtain more accurate data and maps will help reduce model uncertainty. The calibration with one hydrology station increases model uncertainty as it simplifies parameters and phenomena. After considering all uncertainties during the model inputs and parameterisation, the SWAT model provided the simulation result Good for daily

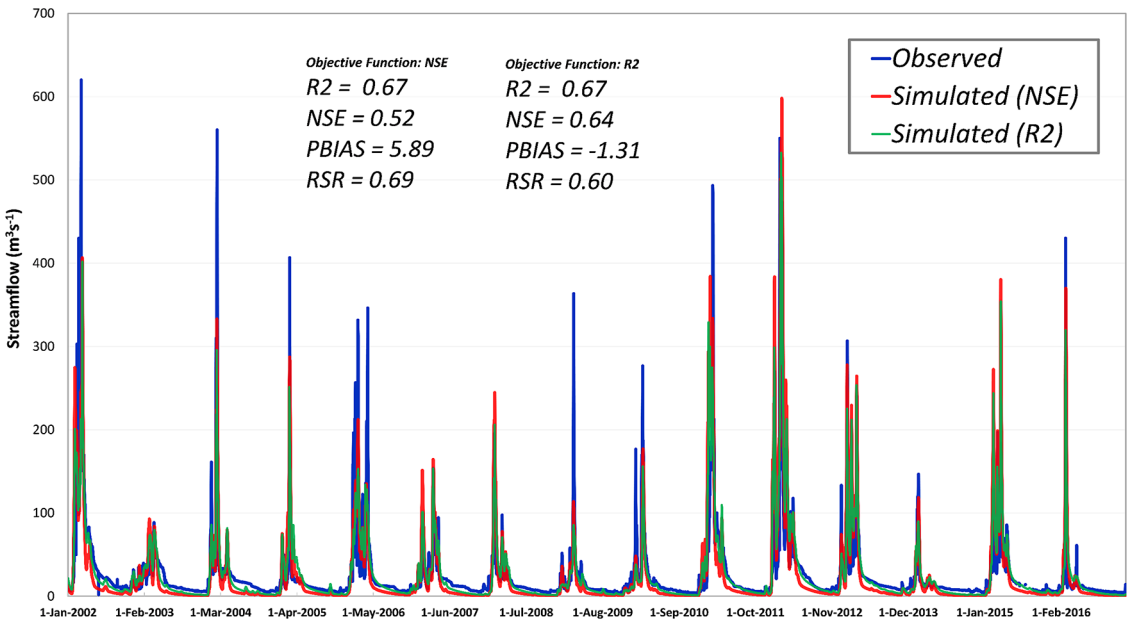

Figure 11. Hydrograph of simulated and observed daily flow using two objective functions for validation period.
NSE indicates Nash-Sutcliffe simulation efficiency; PBIAS, percent bias; RSR, root mean square error.

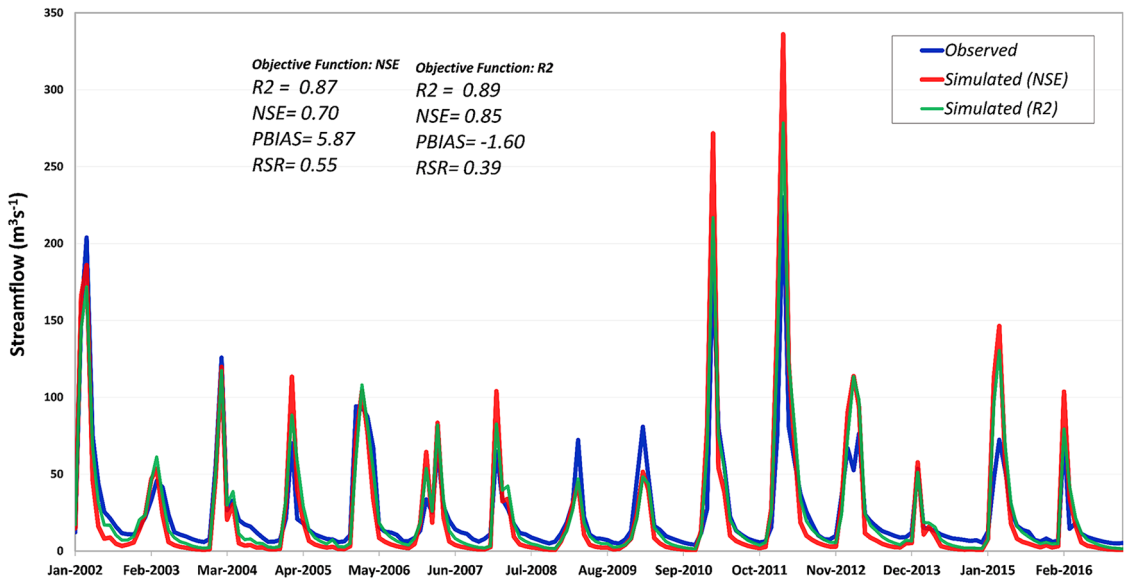

Figure 12. Hydrograph of simulated and observed monthly flow using two objective functions for validation period.
NSE indicates Nash-Sutcliffe simulation efficiency; PBIAS, percent bias; RSR, root mean square error.

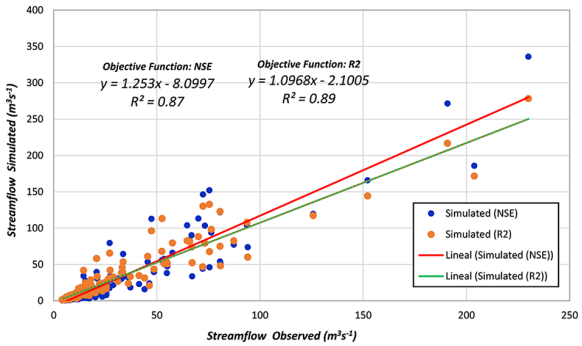

Figure 13. Scatter plot for monthly simulation using two objective functions for validation period.
NSE indicates Nash-Sutcliffe simulation efficiency.

and Very Good for monthly time series using the objective function R^2, for the Tambo River Basin (Table 4).

Finally, the generality of the study findings indicates that they can help in selecting parameters for calibration processes and more applications in other semi-arid areas. The calibrated model may be used to guide water management decisions by stakeholders who have water provision targets to meet, especially in allocating water for agriculture more realistically. Furthermore, the modelling can be applied in planning for the construction of dams in the future, in climate change studies, and in flood risk and disaster management, which will contribute to improved water resources management in the Tambo River Basin.

Table 4. Performance indices from SWAT model calibration and validation using two objective functions.

PERFORMANCE INDEX	OBJECTIVE FUNCTION NSE				OBJECTIVE FUNCTION R^2			
	CALIBRATION		VALIDATION		CALIBRATION		VALIDATION	
	DAILY	MONTH	DAILY	MONTH	DAILY	MONTH	DAILY	MONTH
NSE	0.69 (good)	0.86 (very good)	0.52 (satisfactory)	0.70 (good)	0.65 (good)	0.84 (very good)	0.64 (good)	0.85 (very good)
R^2	0.70 (good)	0.87 (good)	0.67 (good)	0.87 (very good)	0.65 (good)	0.85 (very good)	0.67 (good)	0.89 (very good)
PBIAS	14.7 (good)	14.4 (good)	5.89 (very good)	5.87 (very good)	5.3 (very good)	4.45 (very good)	-1.31 (very good)	-1.60 (very good)
RSR	0.55 (good)	0.38 (very good)	0.69 (satisfactory)	0.55 (good)	0.59 (good)	0.39 (very good)	0.60 (good)	0.39 (very good)

Abbreviations: NSE, Nash-Sutcliffe simulation efficiency; PBIAS, percent bias; RSR, root mean square error; SWAT, Soil and Water Assessment Tool.
Note. The shaded regions in the above table are ones with the best calibration and validation.

Acknowledgements

Streamflow data are from the GeoServer National Water Authority of Peru (ANA) (https://www.ana.gob.pe/). Rainfall and temperature are available from the National Service of Meteorology and Hydrology of Peru (SENAMHI) (https://www.senamhi.gob.pe/).

Author Contributions

JACM: experiment's conception and design, results' technical interpretation, and text writing. TACA: implementation, test, and text writing. SAZM: data providing, results' physical interpretation.

ORCID iD

Juan Adriel Carlos Mendoza https://orcid.org/0000-0003-3568-4388

Supplemental Material

Supplemental material for this article is available online.

REFERENCES

1. Kannan N, White SM, Worrall F, Whelan MJ. Hydrological modelling of a small catchment using SWAT-2000 – ensuring correct flow partitioning for contaminant modelling. *J Hydrol*. 2007;334:64-72. doi:10.1016/j.jhydrol.2006.09.030.
2. Dong W, Lian Y, Zhang Y. *Sustainable Development of Water Resources and Hydraulic Engineering in China: Proceedings for the 2016 International Conference on Water Resource and Hydraulic Engineering*. Cham, Switzerland: Springer International Publishing; 2018. doi:10.1007/978-3-319-61630-8.
3. Suryavanshi S, Pandey A, Chaube UC. Hydrological simulation of the Betwa River basin (India) using the SWAT model. *Hydrol Sci J*. 2017;62:960-978. doi:10.1080/02626667.2016.1271420.
4. Gassman PW, Sadeghi AM, Srinivasan R. Applications of the SWAT model special section: overview and insights. *J Environ Qual*. 2014;43:1-8. doi:10.2134/jeq2013.11.0466.
5. Arnold JG, Srinivasan R, Muttiah RS, Williams JR. Large area hydrologic modeling and assessment part I: model development. *J Am Water Resour As*. 1998;34:73-89. doi:10.1111/j.1752-1688.1998.tb05961.x.
6. Arnold JG, Kiniry JR, Srinivasan R, Williams JR, Haney EB, Neitsch SL. *Input/Output Documentation Soil, Water Assessment Tool*. https://swat.tamu.edu/media/69296/swat-io-documentation-2012.pdf. Published 2012.
7. Neitsch S, Arnold J, Kiniry J, Williams J. *Soil & Water Assessment Tool Theoretical Documentation Version 2009*. College Station, TX: Texas Water Resources Institute; 2011. doi:10.1016/j.scitotenv.2015.11.063.
8. Wagener T, McIntyre N, Lees MJ, Wheater HS, Gupta HV. Towards reduced uncertainty in conceptual rainfall-runoff modelling: dynamic identifiability analysis. *Hydrol Process*. 2003;17:455-476. doi:10.1002/hyp.1135.
9. Sivapalan M, Takeuchi K, Franks SW, et al. IAHS decade on predictions in ungauged basins (PUB), 2003-2012: shaping an exciting future for the hydrological sciences. *Hydrol Sci J*. 2003;48:857-880. doi:10.1623/hysj.48.6.857.51421.
10. Fakult M, Kiel MP. *A Guideline for Hydrologically Consistent Models*. https://nbn-resolving.org/urn:nbn:de:gbv:8-diss-177500. Published 2015.
11. Wu H, Chen B. Evaluating uncertainty estimates in distributed hydrological modeling for the Wenjing River watershed in China by GLUE, SUFI-2, and ParaSol methods. *Ecol Eng*. 2015;76:110-121. doi:10.1016/j.ecoleng.2014.05.014.
12. Abbaspour KC, Johnson CA, van Genuchten MT. Estimating uncertain flow and transport parameters using a Sequential Uncertainty Fitting procedure. *Vadose Zone J*. 2004;3:1340-1352. doi:10.2136/vzj2004.1340.
13. Tapley TD, Waylen PR. Variabilité spatiale des précipitations annuelles et caractère variable de enso dans l'ouest du pérou. *Hydrol Sci J*. 1990;35:429-446. doi:10.1080/02626669009492444.
14. Alegria JF. *The Challenges of Water Resources Management in Peru*. International Water Management Workshop. http://citeseerx.ist.psu.edu/viewdoc/download?doi=10.1.1.485.8798&rep=rep1&type=pdf. Published 2007.
15. ANA. *Water Resource Management Plan for the Caplina-Locumba Basin*. Lima, Peru: Autoridad Nacional Del Agua; 2015.
16. ANA. *Ministry of Agriculture National Institute of Natural Resources Intendency of Water Resources Hydraulic Securing of the Tambo Valley Tomo II Main Report*. Lima, Peru: INRENA, Autoridad Nacional Del Agua; 2005.
17. ANA. *Hydrological Study to Determine the Water Potential of the Tambo and Moquegua River Basins, Through the Development of a Decision Support Model With the Application of WEAP Software: Final Report*. Lima, Peru: Autoridad Nacional Del Agua; 2013.
18. Lavado-Casimiro WS, Felipe O, Silvestre E, Bourrel L. ENSO impact on hydrology in Peru. *Adv Geosci*. 2013;33:33-39. doi:10.5194/adgeo-33-33-2013.
19. ANA. *Moquegua Irrigation Project*. Repositorio Institucional – ANA. MKE. http://repositorio.ana.gob.pe/handle/20.500.12543/4113. Published 1966. Accessed April 24, 2020.
20. Mortensen E, Wu S, Notaro M, et al. Regression-based season-ahead drought prediction for southern Peru conditioned on large-scale climate variables. *Hydrol Earth Syst Sc*. 2018;22:287-303. doi:10.5194/hess-22-287-2018.
21. ANA. *Moquegua Irrigation Technical Data Sheet*. Lima, Peru: INRENA, Autoridad Nacional Del Agua; 2003.
22. ANA. *Monitoring of Surface Water Quality*. Lima, Peru: Autoridad Nacional Del Agua; 2000.
23. MINAM. Geoservidor – El Geoservidor Del MINAM forma parte de la red de información geográfica de América Latina y el Caribe a través del GeoPortal del programa GeoSur. https://www.senamhi.gob.pe/?p=descarga-datos-hidrometeorologicos. Published 2020. Accessed April 24, 2020.
24. FAO. Mapa Mundial de Suelos de FAO/UNESCO| Portal de Suelos de la FAO| Organización de las Naciones Unidas para la Alimentación y la Agricultura. http://www.fao.org/soils-portal/soil-survey/mapas-historicos-de-suelos-y-bases-de-datos/mapa-mundial-de-suelos-de-faounesco/es/. Published 2020. Accessed April 24, 2020.
25. SENAMHI. SENAMHI – Perú. https://senamhi.gob.pe. Published 2020. Accessed April 24, 2020.

26. ANA. Autoridad Nacional del Agua. https://www.ana.gob.pe/. Published 2020. Accessed April 24, 2020.
27. Niraula R, Norman LM, Meixner T, Callegary JB. Multi-gauge calibration for modeling the Semi-Arid Santa Cruz watershed in Arizona-Mexico border area using SWAT [published online ahead of print April 30, 2012]. *Air Soil Water Res*. doi:10.4137/ASWR.S9410.
28. Abbaspour KC, Yang J, Maximov I, et al. Modelling hydrology and water quality in the pre-alpine/alpine Thur watershed using SWAT. *J Hydrol*. 2007;333:413-430. doi:10.1016/j.jhydrol.2006.09.014.
29. Abbaspour KC, Vaghefi SA, Srinivasan R. A guideline for successful calibration and uncertainty analysis for soil and water assessment: a review of papers from the 2016 international SWAT conference. *Water (Switzerland)*. 2018;10:6. doi:10.3390/w10010006.
30. Beven K, Binley A. The future of distributed models: model calibration and uncertainty prediction. *Hydrol Process*. 1992;6:279-298. doi:10.1002/hyp.3360060305.
31. Yang J, Reichert P, Abbaspour KC, Xia J, Yang H. Comparing uncertainty analysis techniques for a SWAT application to the Chaohe Basin in China. *J Hydrol*. 2008;358:1-23. doi:10.1016/j.jhydrol.2008.05.012.
32. Legates DR, McCabe GJ. Evaluating the use of 'goodness-of-fit' measures in hydrologic and hydroclimatic model validation. *Water Resour Res*. 1999;35:233-241. doi:10.1029/1998WR900018.
33. Duan Q, Schaake J, Andréassian V, et al. Model parameter estimation experiment (MOPEX): an overview of science strategy and major results from the second and third workshops. *J Hydrol*. 2006;320:3-17. doi:10.1016/j.jhydrol.2005.07.031.
34. Kouchi DH, Esmaili K, Faridhosseini A, Sanaeinejad SH, Khalili D, Abbaspour KC. Sensitivity of calibrated parameters and water resource estimates on different objective functions and optimization algorithms. *Water (Switzerland)*. 2017;9:384. doi:10.3390/w9060384.
35. Narsimlu B, Gosain AK, Chahar BR, Singh SK, Srivastava PK. SWAT model calibration and uncertainty analysis for streamflow prediction in the Kunwari River Basin, India, using Sequential Uncertainty Fitting. *Environ Processes*. 2015;2:79-95. doi:10.1007/s40710-015-0064-8.
36. Lévesque É, Anctil F, Van Griensven A, Beauchamp N. Evaluation of streamflow simulation by SWAT model for two small watersheds under snowmelt and rainfall. *Hydrol Sci J*. 2008;53:961-976. doi:10.1623/hysj.53.5.961.
37. Li Q, Chen X, Luo Y, Lu ZH, Wang YG. A new parallel framework of distributed SWAT calibration. *J Arid Land*. 2015;7:122-131. doi:10.1007/s40333-014-0041-5.
38. Abbaspour KC, Rouholahnejad E, Vaghefi S, Srinivasan R, Yang H, Kløve B. A continental-scale hydrology and water quality model for Europe: calibration and uncertainty of a high-resolution large-scale SWAT model. *J Hydrol*. 2015;524:733-752. doi:10.1016/j.jhydrol.2015.03.027.
39. Daggupati P, Yen H, White MJ, et al. Impact of model development, calibration and validation decisions on hydrological simulations in West Lake Erie Basin. *Hydrol Process*. 2015;29:5307-5320. doi:10.1002/hyp.10536.
40. Pereira DDR, Martinez MA, de Almeida AQ, Pruski FF, da Silva DD, Zonta JH. Hydrological simulation using SWAT model in headwater basin in Southeast Brazil. *Eng Agric*. 2014;34:789-799. doi:10.1590/S0100-69162014000400018.
41. Marek GW, Gowda PH, Evett SR, et al. Calibration and validation of the SWAT model for predicting daily ET over irrigated crops in the Texas High Plains using lysimetric data. *T ASABE*. 2016;59:611-622. doi:10.13031/trans.59.10926.
42. Moriasi DN, Gitau MW, Pai N, Daggupati P. Hydrologic and water quality models: performance measures and evaluation criteria. *T ASABE*. 2015;58:1763-1785. doi:10.13031/trans.58.10715.
43. Gupta HV, Sorooshian S, Yapo PO. Status of automatic calibration for hydrologic models: comparison with multilevel expert calibration. *J Hydrol Eng*. 1999;4:135-143. doi:10.1061/(asce)1084-0699(1999)4:2(135)
44. Kumar N, Singh SK, Srivastava PK, Narsimlu B. SWAT model calibration and uncertainty analysis for streamflow prediction of the Tons River Basin, India, using Sequential Uncertainty Fitting (SUFI-2) algorithm. *Model Earth Syst Environ*. 2017;3:30. doi:10.1007/s40808-017-0306-z.
45. Moriasi DN, Arnold JG, Van Liew MW, Bingner RL, Harmel RD, Veith TL. Model evaluation guidelines for systematic quantification of accuracy in watershed simulations. *T ASABE*. 2007;50:885-900. doi:10.13031/2013.23153.
46. Fernandez GP, Chescheir GM, Skaggs RW, Amatya DM. Development and testing of watershed-scale models for poorly drained soils. *Trans Am Soc Agric Eng*. 2005;48:639-652. doi:10.13031/2013.18323.
47. Van Liew MW, Arnold JG, Garbrecht JD. Hydrologic simulation on agricultural watersheds: choosing between two models. *Trans Am Soc Agric Eng*. 2003;46:1539-1551. doi:10.13031/2013.15643.
48. Duru U, Arabi M, Wohl EE. Modeling stream flow and sediment yield using the SWAT model: a case study of Ankara River basin, Turkey. *Phys Geogr*. 2018;39:264-289. doi:10.1080/02723646.2017.1342199.
49. Rostamian R, Jaleh A, Afyuni M, et al. Application of a SWAT model for estimating runoff and sediment in two mountainous basins in central Iran. *Hydrol Sci J*. 2008;53:977-988. doi:10.1623/hysj.53.5.977.
50. Xue C, Chen B, Wu H. Parameter uncertainty analysis of surface flow and sediment yield in the Huolin Basin, China. *J Hydrol Eng*. 2014;19:1224-1236. doi:10.1061/(asce)he.1943-5584.0000909.